OPEN ACCESS
International Journal of Innovations in Science & Technology
RESEARCH & INNOVATION DIVISION
IJIST

A Hierarchical Ensemble Deep Learning Framework for Angiographic Blood Vessel Segmentation and Coronary Artery Disease Classification

Abdullah[1], Nizam Ahmad[1], Habib Un Nabi[1], Muhammad Khan[1], Romaan Khan[1], Islam Uddin[2*]

[1]Institute of Computer Science and Information Technology, University of Agriculture Peshawar, Pakistan

[2]Department of Computer Science, Abdul Wali Khan University Mardan, Pakistan

*__Correspondence__: islamuddin@awkum.edu.pk

Citation | Abdullah, Ahmad. N, Nabi. H. U, Khan. M, Khan. R, Uddin. I, "A Hierarchical Ensemble Deep Learning Framework for Angiographic Blood Vessel Segmentation and Coronary Artery Disease Classification", IJIST, Vol. 8 Issue. 5 pp 1938-1965, August 2026

Received | July 26, 2026 **Revised |** Aug 06, 2026 **Accepted |** Aug 06, 2026 **Published |** Aug 15, 2026.

Artificial Intelligence (AI) and deep learning have revolutionized medical image analysis by enabling accurate, efficient, and automated disease diagnosis across diverse healthcare applications. In cardiovascular medicine, these technologies have significantly improved the analysis of coronary angiographic images, supporting early detection and clinical decision-making for coronary artery disease (CAD). However, accurate angiographic blood vessel segmentation and disease classification remain challenging due to low image contrast, brightness inhomogeneity, imaging noise, and the limited feature representation capability of single deep learning models. To address these challenges, this paper proposes a hierarchical ensemble-based deep learning framework for angiographic blood vessel segmentation and coronary artery disease classification. First, Principal Component Analysis (PCA), Contrast Limited Adaptive Histogram Equalization (CLAHE), and the Toggle Contrast Operator (TCO) are employed to enhance angiographic image quality. Secondly, an adaptive Gaussian kernel probability density function (PDF)-based matched filtering technique, followed by entropy-based thresholding, length filtering, and masking, is applied for accurate coronary vessel segmentation. Thirdly, complementary deep features are extracted using EfficientNet-B0, VGG-16, and ResNet-152 and integrated through an ensemble feature fusion strategy. Finally, the fused features are classified using a Softmax classifier. Experimental results demonstrate that the proposed framework achieves an accuracy of 91.23%, precision of 91.84%, sensitivity of 90.97%, specificity of 93.41%, F1-score of 91.40%, MCC of 0.825, Cohen's Kappa of 0.823, and an AUC of 0.951. Comparative evaluation against conventional machine learning and state-of-the-art deep learning models demonstrates that the proposed framework provides superior classification performance, robustness, and diagnostic reliability, "making it a promising computer-aided clinical decision support tool" l for coronary artery disease diagnosis.

Keywords: Coronary Angiography; Blood Vessel Segmentation; Coronary Artery Disease; Ensemble Deep Learning; Feature Fusion; Computer-Aided Diagnosis.

Introduction:

In recent years, artificial intelligence (AI) and deep learning (DL) have rapidly transformed healthcare by enabling intelligent, accurate, and automated analysis of complex medical data [1]. The integration of AI into medical imaging has significantly improved the early detection, diagnosis, prognosis, and treatment planning of various diseases, including cardiovascular disorders, cancer, neurological diseases, and pulmonary abnormalities [2]. Among different imaging modalities, coronary angiography remains the gold standard for visualizing coronary arteries and assessing the severity of coronary artery disease (CAD), one of the leading causes of morbidity and mortality worldwide [3]. Angiographic imaging provides detailed visualization of vascular anatomy, allowing clinicians to identify stenosis, vessel occlusions, and structural abnormalities that are critical for timely clinical intervention [4]. However, manual interpretation of angiographic images is often labor-intensive, time-consuming, and highly dependent on the expertise of interventional cardiologists, leading to inter-observer variability and potential diagnostic inconsistencies [5]. Consequently, the development of intelligent computer-aided diagnosis (CADx) systems based on advanced AI techniques has become an important research direction in cardiovascular medicine [6]. Recent advances in deep convolutional neural networks, transfer learning, ensemble learning, and medical image segmentation have substantially enhanced the capability of automated angiographic image analysis by learning discriminative vascular features directly from image data [7]. These technological developments have improved the accuracy of blood vessel segmentation, lesion detection, and coronary artery disease classification, thereby supporting more reliable clinical decision-making [8]. As a result, AI-driven angiographic image analysis has emerged as a promising approach for improving diagnostic efficiency, reducing clinician workload, and facilitating precision cardiovascular healthcare through robust and automated assessment of coronary vascular abnormalities [9].

Recent studies have demonstrated that deep learning has substantially improved automated coronary angiographic image analysis through advanced vessel segmentation and disease classification techniques [10]. Convolutional neural networks (CNNs), U-Net variants, ResNet, DenseNet, EfficientNet, Vision Transformers (ViTs), and hybrid deep learning architectures have achieved promising performance by learning hierarchical feature representations directly from angiographic images [11]. Furthermore, transfer learning, attention mechanisms, feature fusion, and ensemble learning strategies have enhanced diagnostic accuracy by integrating complementary visual information extracted from multiple network architectures [12]. These developments have contributed to more precise coronary vessel extraction, stenosis detection, and coronary artery disease classification, while reducing dependence on handcrafted image features. Despite these significant advancements, several challenges remain unresolved. Coronary angiographic images frequently exhibit low contrast, brightness inhomogeneity, imaging noise, vessel overlap, and substantial variations in vessel diameter, all of which complicate accurate vessel segmentation and subsequent disease classification [13]. Many existing approaches rely on a single deep learning architecture, limiting their ability to capture diverse and complementary feature representations necessary for robust diagnosis [14]. In addition, numerous studies focus exclusively on either vessel segmentation or disease classification rather than integrating both tasks into a unified framework [15]. Existing segmentation methods often experience degraded performance in challenging clinical images, whereas classification models remain sensitive to segmentation errors and image quality degradation [16]. These limitations reduce model robustness, restrict generalizability across diverse clinical settings, and hinder the practical deployment of automated computer-aided diagnosis systems [17]. Therefore, there remains a critical need for a robust, integrated, and intelligent framework capable of simultaneously enhancing angiographic image quality, accurately segmenting coronary blood vessels, and improving

coronary artery disease classification through complementary deep feature learning [18].

Based on the above-mentioned considerations, this study proposes a hierarchical ensemble-based deep learning framework for angiographic blood vessel segmentation and coronary artery disease classification to address the limitations of existing automated diagnostic approaches. The proposed framework integrates image enhancement, vessel segmentation, deep feature extraction, feature fusion, and disease classification into a unified pipeline, enabling more accurate and robust analysis of coronary angiographic images. Principal Component Analysis (PCA), Contrast Limited Adaptive Histogram Equalization (CLAHE), and the Toggle Contrast Operator (TCO) are employed to improve image quality by enhancing vessel visibility, reducing brightness inhomogeneity, and suppressing imaging noise. An adaptive Gaussian kernel probability density function (PDF)-based matched filtering technique, followed by entropy-based thresholding, length filtering, and masking, is then applied to accurately extract coronary blood vessels while preserving vascular continuity and eliminating non-vascular structures. Three complementary deep learning architectures, namely EfficientNet-B0, VGG-16, and ResNet-152, are utilized to learn diverse feature representations that capture both local and global vascular characteristics. The extracted deep features are integrated through an ensemble feature fusion strategy and subsequently classified using a Softmax classifier to improve diagnostic reliability. The integration of complementary preprocessing, adaptive vessel segmentation, and ensemble deep learning enables the proposed framework to enhance classification robustness, reduce the limitations associated with individual deep learning models, and provide an effective computer-aided decision support system for coronary artery disease diagnosis.

The main contributions of this paper are summarized as follows:

A hierarchical ensemble-based deep learning framework is proposed for automated angiographic blood vessel segmentation and coronary artery disease classification by integrating image enhancement, vessel segmentation, feature extraction, feature fusion, and classification into a unified pipeline.

An adaptive vessel segmentation approach is developed by combining PCA, CLAHE, the Toggle Contrast Operator (TCO), adaptive Gaussian kernel PDF-based matched filtering, and entropy-based thresholding to improve vessel extraction from coronary angiographic images.

An ensemble feature fusion strategy is introduced to integrate complementary deep features extracted from EfficientNet-B0, VGG-16, and ResNet-152, enabling more comprehensive feature representation for disease classification.

A comprehensive evaluation framework is established using multiple performance metrics and comparative analyses to systematically assess the effectiveness and robustness of the proposed method against existing approaches.

The remainder of this paper is organized as follows. Section 2 reviews the related literature. Section 3 presents the proposed methodology, including preprocessing, vessel segmentation, and ensemble-based classification. Section 4 discusses the experimental results and performance evaluation. Finally, Section 5 concludes the study and outlines future research directions.

Related Work:

Artificial intelligence (AI) and deep learning have significantly transformed automated coronary angiographic image analysis by improving blood vessel segmentation and coronary artery disease (CAD) classification. Recent advances in machine learning, convolutional neural networks (CNNs), transfer learning, and ensemble learning have enabled computer-aided diagnosis systems to learn discriminative image features directly from angiographic images, thereby improving diagnostic efficiency and reducing reliance on

manual interpretation. Despite these advances, accurate segmentation and classification remain challenging because coronary angiographic images often exhibit low contrast, imaging noise, vessel overlap, brightness inhomogeneity, and substantial variations in vessel morphology. Consequently, numerous studies have proposed different segmentation and classification strategies to address these challenges, each demonstrating specific strengths and limitations. Among the traditional vessel segmentation approaches, a multiscale Gabor filter combined with a Gaussian filter was proposed to enhance vascular structures in coronary angiographic images. The proposed method achieved high classification accuracy and specificity, demonstrating its capability to distinguish vessel and non-vessel pixels effectively. Nevertheless, the relatively lower sensitivity and Dice coefficient indicate that the method encounters difficulties in accurately extracting thin vessels and preserving vessel continuity. Similarly, [19] introduced a multiscale region-growing algorithm for coronary vessel segmentation. Although the method achieved satisfactory mean precision, the considerable variation in Dice coefficients across different datasets suggests inconsistent segmentation performance under varying imaging conditions. These observations indicate that conventional filtering and region-growing techniques remain sensitive to image quality degradation and often struggle to provide reliable vessel extraction in complex coronary angiograms.

Recent deep learning methods have substantially improved automated coronary artery disease classification by learning hierarchical feature representations directly from medical images. In [20], DenseNet121 was employed to classify coronary artery disease and achieved an average accuracy of 93.7% with a high F1-score, demonstrating the effectiveness of densely connected convolutional networks for cardiovascular image analysis. The relatively larger dataset used in the study also enhanced the model's generalization capability. Likewise, [21] proposed AngioNet CNN for coronary vessel segmentation and reported excellent pixel accuracy, sensitivity, specificity, and Dice score, indicating robust vessel extraction performance. Despite these encouraging results, deep learning models generally require large annotated datasets and considerable computational resources for effective training. Moreover [22] single-network architectures may not adequately capture complementary feature representations, thereby limiting robustness when angiographic images contain imaging noise, low contrast, or highly complex vascular structures. Several studies have attempted to improve segmentation and classification performance using alternative methodologies. In [23], a threshold-based segmentation technique achieved high accuracy and specificity; however, its relatively moderate sensitivity indicates limited capability in detecting small or low-contrast vessels. Similarly, [24] integrated CLAHE with a U-Net architecture to enhance vessel contrast before segmentation. Although the method improved segmentation quality by combining multiscale feature learning with image enhancement, the reported Dice coefficient suggests that segmentation performance can still deteriorate under challenging angiographic conditions. Furthermore, [25] proposed an SVM-based classifier integrated with UDMA for coronary image analysis and achieved satisfactory classification accuracy. Nevertheless, the incorporation of synthetic angiographic images to enlarge the dataset may introduce distribution bias, potentially affecting the model's generalization to real clinical scenarios [26].

The existing studies have demonstrated significant progress in coronary angiographic blood vessel segmentation and coronary artery disease classification through conventional image processing, machine learning, and deep learning techniques. Nevertheless, several important challenges remain unresolved. Traditional segmentation methods are highly sensitive to low image contrast, brightness inhomogeneity, and imaging noise, resulting in incomplete vessel extraction and reduced segmentation accuracy. Although deep learning-based approaches have improved diagnostic performance, most rely on a single network

architecture, limiting their ability to learn complementary feature representations from complex angiographic images. Furthermore, many existing studies address vessel segmentation and disease classification as separate tasks, while limited attention has been given to developing an integrated framework that combines image enhancement, adaptive vessel segmentation, ensemble feature fusion, and automated classification within a unified pipeline. These limitations reduce the robustness, generalizability, and clinical applicability of existing computer-aided diagnosis systems. Therefore, there is a need for a comprehensive and robust ensemble-based framework capable of enhancing angiographic image quality, accurately segmenting coronary blood vessels, and improving coronary artery disease classification through complementary deep feature learning.

Proposed Methodology:

This section presents the proposed hierarchical ensemble-based deep learning framework for automated angiographic blood vessel segmentation and coronary artery disease classification. The framework integrates image preprocessing, adaptive vessel segmentation, deep feature extraction, ensemble feature fusion, and classification into a unified diagnostic pipeline. Initially, angiographic images are enhanced to improve vessel visibility and suppress imaging artifacts. The segmented vessel images are subsequently processed by multiple deep learning models to extract complementary feature representations, which are fused for accurate disease classification.

Proposed Framework Architecture:

The proposed hierarchical ensemble-based deep learning framework consists of five sequential stages designed to improve the accuracy and robustness of automated coronary artery disease (CAD) diagnosis from angiographic images [27]. The framework begins with the acquisition of raw coronary angiographic images, which serve as the input for subsequent processing. In the first stage, image preprocessing is performed using Principal Component Analysis (PCA), Contrast Limited Adaptive Histogram Equalization (CLAHE), and the Toggle Contrast Operator (TCO) to enhance vessel visibility, improve image contrast, reduce brightness inhomogeneity, and suppress imaging artifacts [28]. The enhanced images are then processed by an adaptive vessel segmentation module that combines adaptive Gaussian kernel probability density function (PDF)-based matched filtering, entropy-based thresholding, and length filtering with masking to accurately extract coronary blood vessels while eliminating background noise and irrelevant structures. The segmented vessel images are subsequently provided to three complementary deep learning models, namely EfficientNet-B0, VGG-16, and ResNet-152, where each network independently learns discriminative feature representations from different architectural perspectives. The extracted deep features are integrated through an ensemble feature fusion strategy based on feature concatenation and dimensionality reduction using PCA to generate a compact and informative feature vector. Finally, the fused features are classified using a Softmax classifier, which computes the probability scores for normal and CAD classes and produces the final diagnostic decision. The integration of image enhancement, adaptive vessel segmentation, complementary feature extraction, and ensemble learning enables the proposed framework to provide a robust and reliable computer-aided diagnosis system for coronary artery disease classification. The architecture of the proposed hierarchical ensemble-based deep learning framework is illustrated in Figure 1.

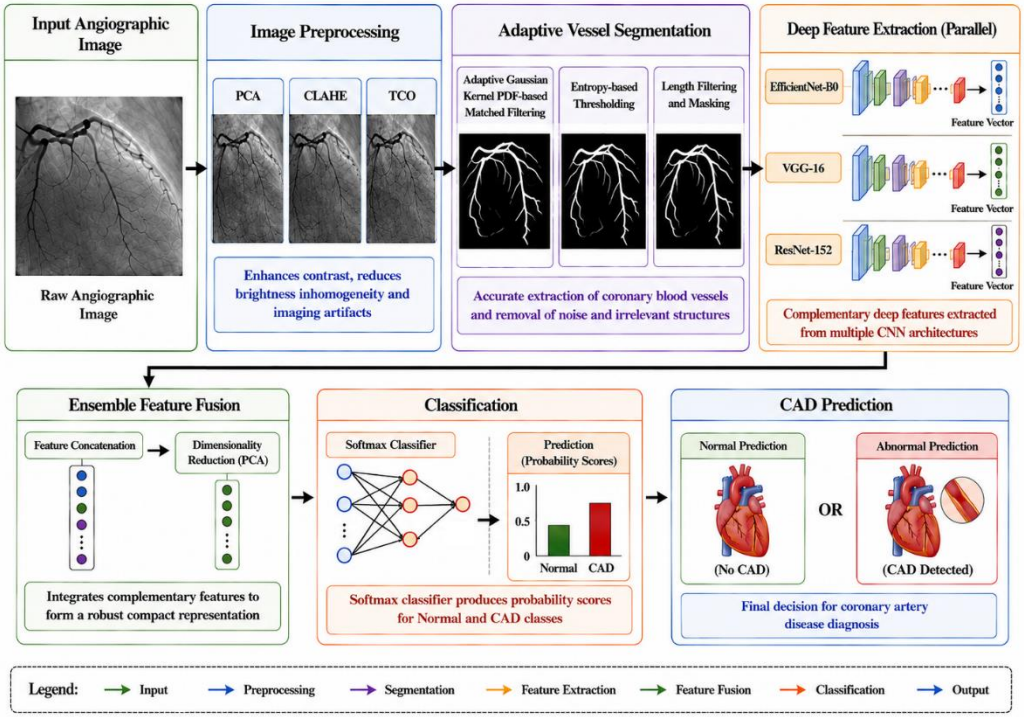

Figure 1. Architecture of the Proposed Hierarchical Ensemble-Based Deep Learning Framework

Coronary Angiographic Image Dataset:

The proposed hierarchical ensemble-based deep learning framework was developed and evaluated using two complementary datasets: (i) a coronary angiographic image dataset for blood vessel segmentation and coronary artery disease classification, and (ii) a heart disease clinical dataset for evaluating the classification performance of the proposed framework. The combination of imaging and clinical information enables a comprehensive assessment of the proposed computer-aided diagnosis system. The coronary angiographic image dataset was collected from Hayatabad Medical Complex (HMC) and Khyber Teaching Hospital (KTH), Peshawar, Pakistan. The dataset consists of 1,600 coronary angiographic images, equally distributed among four clinically relevant categories, namely Normal, Reduced Blood Flow, Blocked Vessels, and Narrow Vessels, with 400 images in each category. This balanced distribution minimizes classification bias and ensures adequate representation of each class during model training and evaluation [29]. The detailed distribution of the coronary angiographic image dataset is presented in Table 1.

Table 1. Distribution of the Coronary Angiographic Image Dataset

S. No.	Category	Number of Images
1	Normal	400
2	Reduced Blood Flow	400
3	Blocked Vessels	400
4	Narrow Vessels	400
Total	**Four Categories**	**1,600**

To improve the robustness and generalization capability of the proposed framework, several data augmentation techniques, including image rotation, horizontal flipping, and random cropping, were applied during the training stage. These augmentation strategies increase image diversity while preserving clinically relevant vascular structures and reducing the possibility of model overfitting. Angiographic images were acquired using standard coronary angiography procedures and anonymized before analysis to preserve patient

confidentiality. Ethical approval for the study was obtained from the Institutional Review Board (IRB) of the participating hospitals, and all personally identifiable information was removed before data processing to ensure compliance with institutional ethical standards and applicable data protection regulations [30].

A benchmark heart disease clinical dataset containing 1,026 patient records was additionally utilized to evaluate the classification capability of the proposed framework. The dataset comprises 498 normal cases and 528 coronary artery disease cases, providing a balanced distribution for binary classification. Each patient record contains demographic information, physiological measurements, laboratory findings, and cardiovascular risk factors associated with coronary artery disease. The dataset includes 13 clinical features, namely Age, Sex, Chest Pain Type (Cp), Resting Blood Pressure (Trestbps), Serum Cholesterol (Chol), Fasting Blood Sugar (Fbs), Resting Electrocardiographic Results (Restecg), Maximum Heart Rate Achieved (Thalach), Exercise-Induced Angina (Exang), ST Depression (Oldpeak), Slope of the Peak Exercise ST Segment (ST_Slope), Number of Major Vessels (Ca), and Thalassemia (Thal). The target variable indicates the presence or absence of coronary artery disease, where 0 denotes no disease and 1 denotes disease [31]. A summary of the heart disease clinical dataset, including the class distribution and feature descriptions, is presented in Table 2.

Table 2. Summary of the Heart Disease Clinical Dataset

Description	Feature	Range / Value
Total Samples	—	**1,026**
No Disease Cases	Target = 0	**498**
Disease Cases	Target = 1	**528**
Age (Years)	Age	28–78
Sex (1 = Male, 0 = Female)	Sex	0–1
Chest Pain Type	Cp	0–3
Serum Cholesterol (mg/dL)	Chol	126–264
Resting Electrocardiographic Results	Restecg	0–2
Resting Blood Pressure (mmHg)	Trestbps	94–200
Slope of Peak Exercise ST Segment	ST_Slope	0–2
Fasting Blood Sugar (>120 mg/dL)	Fbs	0–1
Exercise-Induced Angina	Exang	0–1
ST Depression Induced by Exercise	Oldpeak	0–6.2
Maximum Heart Rate Achieved	Thalach	71–202
Number of Major Vessels	Ca	0–4
Thalassemia	Thal	0–3
Target Variable	Target	**0 = No Disease, 1 = Disease**

Ensemble Deep Learning Framework:

The proposed framework employs an ensemble deep learning strategy that integrates three complementary convolutional neural network (CNN) architectures, namely EfficientNet-B0, VGG-16, and ResNet-152, to improve the accuracy and robustness of coronary artery disease classification. Each architecture is selected for its unique learning capability and contribution to feature representation. EfficientNet-B0 utilizes compound scaling to achieve an optimal balance between classification accuracy and computational efficiency while maintaining a relatively small number of trainable parameters. VGG-16 provides a simple and uniform network architecture that effectively extracts hierarchical texture and structural features from coronary angiographic images. ResNet-152 employs deep residual learning to capture high-level semantic information while mitigating the vanishing gradient problem, thereby improving feature representation for complex vascular

structures. Rather than relying on a single network architecture, the proposed framework integrates the complementary strengths of these three CNN models through an ensemble feature learning strategy. Following image preprocessing and vessel segmentation, the segmented coronary vessel images are independently processed by EfficientNet-B0, VGG-16, and ResNet-152 to extract diverse and discriminative deep feature representations. The extracted features are subsequently combined using an ensemble feature fusion approach to generate a compact and informative feature vector. Finally, the fused feature vector is provided to a Softmax classifier, which computes the probability scores for each diagnostic class and produces the final prediction as either Normal or Abnormal[32]. The overall workflow of the ensemble deep learning framework is illustrated in Figure 2.

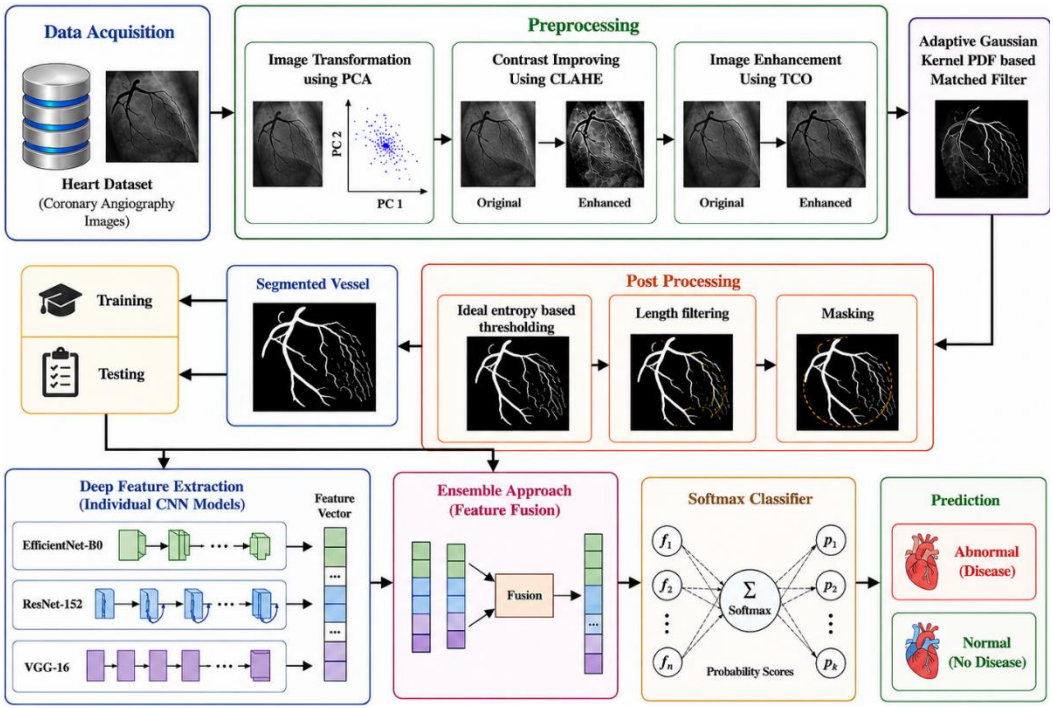

Figure 2. Ensemble Learning Framework for Coronary Artery Disease Classification

Image Contrast Improvement:

Coronary angiographic images frequently exhibit low contrast, non-uniform illumination, imaging noise, and intensity variations that obscure coronary vessel boundaries and adversely affect the performance of automated segmentation and classification algorithms. Consequently, an effective image enhancement strategy is essential to improve vessel visibility while preserving fine anatomical structures. The proposed framework employs a sequential image contrast improvement pipeline comprising Principal Component Analysis (PCA), Contrast Limited Adaptive Histogram Equalization (CLAHE), the Toggle Contrast Operator (TCO), and adaptive Gaussian kernel probability density function (PDF)-based matched filtering. These complementary preprocessing techniques progressively enhance image quality, strengthen vascular structures, and suppress background interference, thereby providing reliable inputs for subsequent vessel segmentation and deep feature extraction [33].

Initially, the RGB coronary angiographic image is transformed into a grayscale representation using Principal Component Analysis (PCA), which projects the original image onto a lower-dimensional feature space while preserving the maximum variance and minimizing redundant information. This transformation reduces computational complexity and retains the most discriminative image characteristics required for subsequent processing. As presented in Eq. (1), the PCA transformation is formulated as:

$$Y = W^T(X - \mu) \quad (1)$$

where Xdenotes the input RGB image, μrepresents the mean image vector, $W$is the projection matrix consisting of the principal eigenvectors, and $Y$is the transformed grayscale image.

Following grayscale conversion, the probability distribution of gray-level intensities is computed to estimate the occurrence frequency of individual pixel values. As defined in Eq. (2), the probability distribution is calculated as:

$$P(g_n) = \frac{k_n}{K} \quad (2)$$

Where $P(g_n)$, represents the probability of occurrence of gray level g_n, k_n, denotes the number of pixels having gray level g_n, and K, is the total number of pixels in the image. Based on this probability distribution, the cumulative distribution function (CDF) is subsequently determined to establish the gray-level transformation required for adaptive histogram equalization. The cumulative probability is computed according to Eq. (3):

$$C(g_n) = \sum_{j=0}^{n} P\left(g_j\right) \quad (3)$$

Where $C(g_n)$, denotes the cumulative distribution function corresponding to gray level g_n. The CDF enables adaptive redistribution of image intensities while preserving important vascular information.

Unlike conventional histogram equalization, which performs global contrast enhancement and may amplify image noise, Contrast Limited Adaptive Histogram Equalization (CLAHE) enhances local contrast by independently processing small neighboring image regions. This localized enhancement significantly improves the visibility of coronary vessels while preventing excessive amplification of homogeneous background regions [34]. The interpolation between adjacent image blocks is performed using Eq. (4):

$$q' = (1 - \delta)M_1(q) + \delta M_2(q) \quad (4)$$

Where q'denotes the interpolated gray value at location q, $M_1(q)$and $M_2(q)$, represent the gray-level mapping functions of two neighboring regions, and $\delta$is the interpolation coefficient satisfying $0 \leq \delta \leq 1$. This interpolation produces smooth transitions between neighboring regions and effectively eliminates boundary artifacts after local histogram equalization.

Although CLAHE substantially enhances local image contrast, coronary angiographic images often continue to exhibit brightness inhomogeneity and weak vessel boundaries, particularly in peripheral vascular regions. To address this limitation, the proposed framework employs the Toggle Contrast Operator (TCO) as a morphological enhancement technique that adaptively combines dilation and erosion operations according to local neighborhood characteristics [35]. The TCO selectively modifies pixel intensities to strengthen vessel boundaries, preserve vascular continuity, and suppress non-vascular structures, thereby generating a more reliable image for vessel enhancement. The enhanced angiographic image is subsequently processed using an adaptive Gaussian kernel probability density function (PDF)-based matched filtering technique to further emphasize coronary vessel structures while suppressing background noise. Since the cross-sectional intensity profile of coronary vessels closely resembles a Gaussian distribution, the matched filter produces strong responses along vessel centerlines while minimizing responses from surrounding tissues. The adaptive Gaussian kernel is formulated according to Eq. (5):

$$G(x, y) = -\exp\left(-\frac{x^2}{2\sigma^2}\right), \quad |y| \leq \frac{L}{2} \quad (5)$$

Where Ldenotes the filter length and σcontrols the Gaussian spread corresponding to vessel width. The matched filter response is subsequently obtained by convolving the enhanced image with the adaptive Gaussian kernel, as expressed in Eq. (6):

$$R(x, y) = I(x, y) * G(x, y) \quad (6)$$

Where $I(x, y)$, represents the enhanced angiographic image, $G(x, y)$, is the adaptive Gaussian kernel, and $R(x, y)$, denotes the matched filter response. To ensure consistent enhancement of vessels with different orientations, the maximum response across all filter directions is selected according to Eq. (7):

$$R_{\max}(x, y) = \max_{i=1}^{N}\{R_i(x, y)\} \quad (7)$$

where $R_i(x, y)$denotes the matched filter response corresponding to the i^{th}orientation and $N$is the total number of filter orientations. Finally, the selected response is normalized using Eq. (8).

$$R_n(x, y) = \frac{R_{\max}(x,y) - R_{\min}}{R_{\max} - R_{\min}} \quad (8)$$

Where $R_n(x, y)$, represents the normalized vessel enhancement image, while $R_{\max}$, and $R_{\min}$, denote the maximum and minimum filter responses, respectively. This normalization suppresses residual background noise, enhances vessel continuity, and generates a uniformly enhanced angiographic image that serves as an effective input for the entropy-based thresholding and subsequent post-processing stages.

Post-processing:

Although the adaptive Gaussian kernel probability density function (PDF)-based matched filtering significantly enhances coronary vessel structures, the resulting response image may still contain isolated noisy pixels, fragmented vessel segments, and small non-vascular objects caused by image noise, intensity variations, and background artifacts. Such imperfections may adversely affect the accuracy of vessel segmentation and subsequent disease classification. Therefore, the proposed framework incorporates a post-processing stage to refine the enhanced vessel image before deep feature extraction. This stage consists of three consecutive operations: entropy-based thresholding, length filtering, and masking, each contributing to the generation of an accurate and continuous coronary vessel map.

Initially, entropy-based thresholding is employed to automatically determine the optimal threshold that separates vessel pixels from the background according to the statistical distribution of gray-level intensities. Unlike fixed thresholding methods, entropy-based thresholding adaptively maximizes the information content between the foreground and background regions, thereby producing more reliable vessel segmentation under varying illumination conditions. As expressed in Eq. (9), the total image entropy is computed as:

$$H(T) = -\sum_{i=0}^{T} P(i) \log P(i) - \sum_{i=T+1}^{L-1} P(i) \log P(i) \quad (9)$$

Where $H(T)$, denotes the total entropy corresponding to threshold T, $P(i)$, represents the probability of occurrence of gray level i, and L, is the total number of gray levels. The optimal threshold is selected by maximizing the entropy, enabling effective separation of coronary vessels from the surrounding background.

Following thresholding, length filtering is applied to remove isolated connected components and short vessel-like structures that do not correspond to actual coronary arteries. This operation preserves elongated vascular branches while eliminating small artifacts generated during image enhancement and thresholding. Consequently, the continuity of the coronary vascular tree is significantly improved without affecting the primary vessel structures. Finally, a mask operation is performed to retain only the anatomical region of interest by eliminating pixels located outside the coronary angiographic field. This operation suppresses residual background structures, imaging artifacts, and irrelevant anatomical regions that may interfere with subsequent feature extraction. The combination of entropy-based thresholding, length filtering, and masking produces a refined vessel segmentation map with improved continuity, reduced false-positive responses, and

enhanced structural integrity. The resulting segmented coronary vessels are subsequently used as the input for the ensemble deep learning framework, enabling accurate feature extraction and robust coronary artery disease classification.

Ideal entropy Thresholding:

Following the post-processing stage, the enhanced coronary vessel response image is converted into a binary segmentation map using an ideal entropy-based thresholding technique. Although the adaptive Gaussian matched filter effectively enhances vascular structures, the enhanced image still contains intensity variations between vessel and background regions. Consequently, an adaptive threshold selection strategy is required to accurately distinguish coronary vessels while preserving fine vascular branches. Unlike conventional thresholding methods that rely solely on pixel intensity values, the proposed method incorporates the Gray-Level Co-occurrence Matrix (GLCM) to exploit the spatial relationship between neighboring pixels. The use of GLCM enables more reliable discrimination between vessel and background regions by considering local texture characteristics in addition to intensity information.

Initially, the gray-level co-occurrence matrix is constructed from the enhanced vessel image. As shown in Eq. (10), the co-occurrence matrix represents the frequency with which neighboring gray-level pairs occur throughout the image.

$$CM(a, b) = \sum_{u=1}^{P} \sum_{v=1}^{Q} \beta \qquad (10)$$

Where $CM(a, b)$, denotes the gray-level co-occurrence matrix corresponding to gray levels a, and b, P, and Q, represent the image dimensions, and β, is an indicator function describing the spatial relationship between neighboring pixels.

The indicator function used to construct the co-occurrence matrix is defined according to Eq. (11):

$$\beta = \begin{cases} 1, & R(u, v) = a \ \wedge \ R(u, v+1) = b \\ 1, & R(u, v) = a \ \wedge \ R(u, +1v) = b \\ 0, & \text{otherwise} \end{cases} \qquad (11)$$

Where $R(u, v)$, denotes the gray-level intensity at pixel location (u, v), while $a$and $b$represent neighboring gray levels.

The co-occurrence matrix is subsequently normalized to estimate the probability distribution of neighboring gray-level pairs. As expressed in Eq. (12):

$$P(a, b) = \frac{CM(a,b)}{\sum_a \sum_b CM(a,b)} \qquad (12)$$

Where $P(a, b)$, denotes the normalized co-occurrence probability.

Based on the normalized co-occurrence matrix, the image is partitioned into vessel and background regions using an adaptive entropy criterion. The cumulative probability associated with the selected threshold is computed according to Eq. (13):

$$W(T) = \sum_{a=0}^{T} \sum_{b=0}^{T} P\,(a, b) \qquad (14)$$

Where T, denotes the threshold separating vessel and background pixels.

Finally, the optimal threshold is determined by maximizing the entropy of the segmented image, producing an accurate binary vessel map while preserving fine coronary branches and suppressing residual background structures. The resulting binary segmentation provides a reliable input for the subsequent length filtering and masking operations.

Heart Diseases Classification:

The refined coronary vessel image obtained after image enhancement and post-processing is provided as the input to the proposed heart disease classification framework. To improve feature representation and classification robustness, the proposed framework

employs an ensemble deep learning strategy that integrates three complementary convolutional neural networks, namely VGG-16, ResNet-152, and EfficientNet-B0. Each network independently extracts discriminative features from segmented coronary vessels according to its architectural characteristics. The extracted feature vectors are subsequently fused and supplied to a Softmax classifier to determine the final disease category. The overall classification framework improves feature diversity, enhances classification robustness, and reduces the limitations associated with individual deep learning models.

VGG-16 is employed to extract hierarchical texture and structural features from segmented coronary vessel images. The network utilizes stacked 3 × 3 convolutional layers followed by pooling operations to progressively learn vessel edges, bifurcations, and morphological characteristics associated with coronary artery disease. The architecture of the VGG-16 feature extraction network adopted in the proposed framework is illustrated in Figure 3.

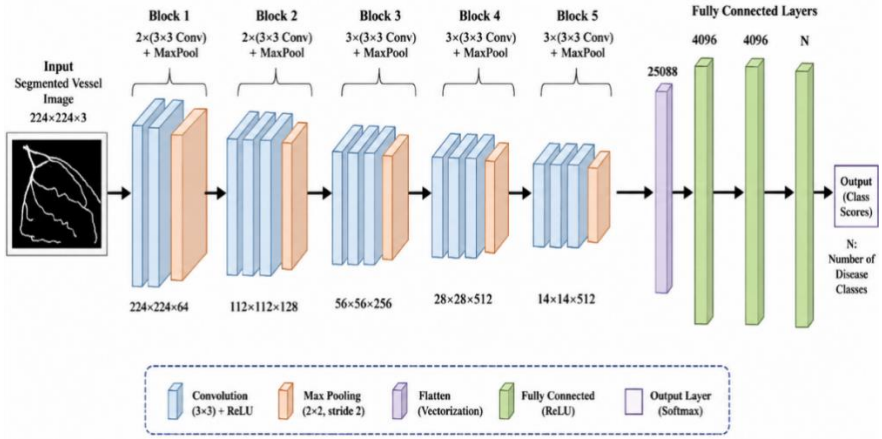

Figure 3. Architecture of the VGG-16 Feature Extraction Network

ResNet-152 complements the features extracted by VGG-16 through deep residual learning, enabling effective optimization of a very deep network while mitigating the vanishing gradient problem. The residual learning mechanism enhances semantic feature extraction from complex coronary vessel structures and is expressed as

$$F(x) = H(x) - x \tag{15}$$

where $F(x)$, denotes the residual mapping, $H(x)$, is the desired transformation, and x, represents the input feature map.

EfficientNet-B0 is incorporated to improve computational efficiency while maintaining high feature representation capability through compound network scaling. The architecture, shown in Figure 4, simultaneously optimizes network depth, width, and input resolution, enabling accurate feature extraction with fewer trainable parameters.

The compound scaling strategy is defined as:

$$D = \alpha^{\psi},\ W = \beta^{\psi},\ R = \gamma^{\psi} \tag{16}$$

Where D, W, and R, denote the network depth, width, and input resolution, respectively, while ψ, is the compound scaling coefficient.

The deep feature vectors generated by VGG-16, ResNet-152, and EfficientNet-B0 are concatenated to form a unified feature representation that combines complementary texture, structural, and semantic information. The fused feature vector is subsequently provided to a Softmax classifier, which estimates the posterior probability of each disease category and assigns the image to the class with the highest probability. The Softmax function is expressed as:

$$P_i = \frac{e^{z_i}}{\sum_{j=1}^{C} e^{z_j}} \quad (17)$$

Where $P_i$denotes the predicted probability of the i^{th}disease class, $z_i$represents the corresponding output score, and C, is the total number of disease classes. Integrating complementary feature representations prior to classification improves feature discrimination, enhances classification robustness, and enables reliable automated coronary artery disease diagnosis.

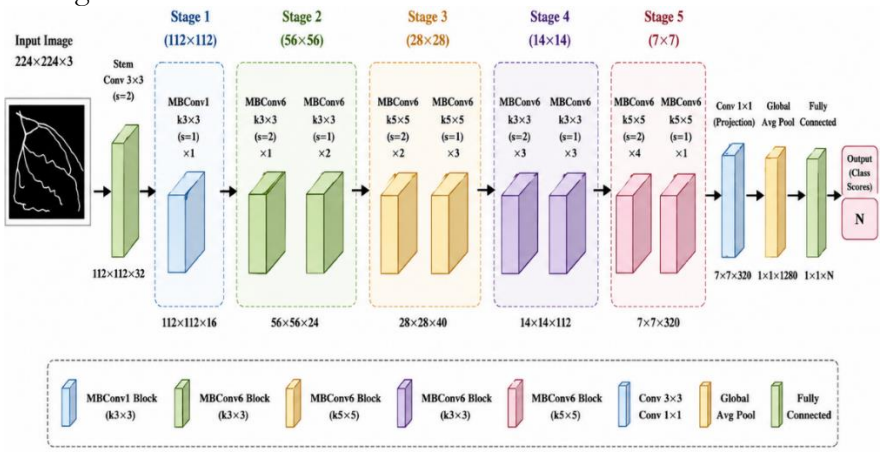

Figure 4 Architecture of the EfficientNet-B0 Feature Extraction Network

Performance Evaluation Metrics:

The performance of the proposed ensemble deep learning framework was evaluated using several widely adopted classification metrics to comprehensively assess its diagnostic capability for coronary artery disease prediction. The evaluation was performed using the confusion matrix, which consists of True Positives (TP), True Negatives (TN), False Positives (FP), and False Negatives (FN) [36]. These four outcomes provide the basis for calculating Accuracy (ACC), Sensitivity (SN), Specificity (SP), Precision (PRE), F1-score, Matthews Correlation Coefficient (MCC), and the Area Under the Receiver Operating Characteristic Curve (AUC). Collectively, these metrics provide a comprehensive assessment of classification accuracy, diagnostic reliability, and the discriminative capability of the proposed framework [37].

Classification accuracy measures the proportion of correctly classified samples among all testing instances and is computed as:

$$\text{ACC} = \frac{TP+TN}{TP+TN+FP+FN} \quad (18)$$

Where $TP$and TNdenote correctly classified positive and negative samples, respectively, while $FP$and FN, represent false positive and false negative predictions.

Sensitivity (SN), also referred to as the true positive rate or recall, evaluates the ability of the proposed framework to correctly identify patients with coronary artery disease. It is calculated as:

$$\text{SN} = \frac{TP}{TP+FN} \quad (19)$$

where a higher sensitivity indicates improved detection of diseased cases.

Specificity (SP) measures the capability of the proposed model to correctly classify normal subjects and is expressed as:

$$\text{SP} = \frac{TN}{TN+FP} \quad (20)$$

Where higher specificity reflects a lower false-positive rate.

Precision (PRE) quantifies the reliability of positive predictions by measuring the proportion of correctly predicted disease cases among all positive predictions and is defined

as:

$$\text{PRE} = \frac{TP}{TP+FP} \quad (21)$$

The F1-score provides a balanced evaluation of Precision and Sensitivity by computing their harmonic mean, particularly when the class distribution is imbalanced. It is computed as:

$$\text{F1} = 2 \times \frac{\text{PRE} \times \text{SN}}{\text{PRE} + \text{SN}} \quad (22)$$

To provide a balanced assessment of classification performance, the Matthews Correlation Coefficient (MCC) was also employed. MCC considers all four elements of the confusion matrix and is calculated as:

$$\text{MCC} = \frac{TP \times TN - FP \times FN}{\sqrt{(TP+FP)(TP+FN)(TN+FP)(TN+FN)}} \quad (23)$$

Where the MCC value ranges from −1 to +1, with +1 indicating perfect classification, 0 representing random prediction, and −1 indicating complete disagreement between predicted and actual classes.

Furthermore, the discriminative capability of the proposed framework was evaluated using the Area Under the Receiver Operating Characteristic Curve (AUC). The AUC measures the classifier's ability to distinguish between disease and normal classes across different decision thresholds and is defined as:

$$\text{AUC} = \int_0^1 T\,PR(FPR)\,d(FPR) \quad (24)$$

Where TPR, denotes the true positive rate (Sensitivity) and FPR, represents the false positive rate $\left(FPR = \frac{FP}{FP+TN}\right)$. An AUC value closer to 1.0 indicates superior discriminative performance and demonstrates the robustness of the proposed ensemble deep learning framework.

The combination of these evaluation metrics provides a comprehensive and objective assessment of the proposed framework by simultaneously evaluating overall classification accuracy, diagnostic sensitivity, specificity, prediction reliability, correlation, and discriminative capability, thereby ensuring a reliable evaluation of coronary artery disease classification performance.

Experimental Results and Analysis:

This section presents the experimental evaluation of the proposed ensemble deep learning framework for coronary artery disease classification using coronary angiographic images. Initially, the experimental environment, including hardware, software, and implementation details, is described. Subsequently, the hyperparameter configuration adopted for model training is presented. The segmentation performance of the proposed image enhancement framework is then evaluated, followed by a comprehensive analysis of heart disease classification performance. Comparative experiments with existing state-of-the-art methods and an ablation study are conducted to validate the contribution of each framework component. Finally, the overall findings and clinical implications of the proposed framework are discussed.

Experimental Environment:

The proposed ensemble deep learning framework was implemented and evaluated using a high-performance computing environment to ensure efficient model training, inference, and experimental reproducibility. The implementation was carried out using the Python programming language together with the TensorFlow and Keras deep learning libraries. Image preprocessing, vessel enhancement, segmentation, and data visualization were performed using OpenCV, NumPy, Pandas, Scikit-learn, and Matplotlib. These software libraries provide efficient implementations for image processing, numerical computation, model optimization, and performance evaluation. To accelerate deep learning

training, all experiments were executed on a workstation equipped with an NVIDIA graphics processing unit (GPU) supporting CUDA and cuDNN for parallel computation. The proposed framework was trained using GPU acceleration, significantly reducing computational time while improving training efficiency for the ensemble deep learning architecture. During experimentation, the same hardware and software configuration was maintained to ensure consistency and reproducibility of the obtained results. The experimental environment was configured to support all stages of the proposed framework, including coronary angiographic image preprocessing, adaptive vessel enhancement, entropy-based segmentation, deep feature extraction using VGG-16, ResNet-152, and EfficientNet-B0, ensemble feature fusion, and heart disease classification. All experiments were conducted under identical computational conditions to ensure a fair evaluation of the proposed framework and facilitate comparison with existing methods. The detailed hardware and software specifications used during the experimental evaluation are summarized in Table 3.

Table 3. Hardware and software configuration used for experimental evaluation.

Component	Specification
Processor (CPU)	Intel® Core™ i9-14900K (24 Cores, 32 Threads)
Graphics Processing Unit (GPU)	NVIDIA GeForce RTX 4090 (24 GB GDDR6X)
System Memory (RAM)	64 GB DDR5
Storage	2 TB NVMe SSD
Operating System	Windows 11 Pro (64-bit)
Programming Language	Python 3.11
Deep Learning Framework	TensorFlow 2.16 with Keras
Machine Learning Library	Scikit-learn
Image Processing Library	OpenCV
Scientific Computing	NumPy, Pandas
Data Visualization	Matplotlib
GPU Computing Platform	CUDA 12.x
GPU Acceleration Library	cuDNN 9.x
Development Environment	Jupyter Notebook

Hyperparameter Configuration:

The selection of appropriate hyperparameters plays a critical role in the training stability and predictive performance of deep learning models. To achieve robust convergence and improve the generalization capability of the proposed ensemble framework, extensive preliminary experiments were conducted to determine the optimal training configuration. The hyperparameters were selected by considering training convergence, classification accuracy, computational efficiency, and model stability while minimizing overfitting. The proposed ensemble framework was trained using the Adam optimizer, which provides efficient adaptive learning and fast convergence during backpropagation. An initial learning rate of 0.0001 was adopted to ensure stable weight updates throughout the optimization process. The batch size was fixed at 32, providing an effective balance between computational efficiency and gradient estimation accuracy. The training process was performed for 100 epochs, allowing the network to sufficiently learn representative features from the coronary angiographic images while maintaining stable convergence. The Rectified Linear Unit (ReLU) activation function was employed in all hidden layers because of its computational simplicity and ability to mitigate the vanishing gradient problem. The output layer utilized the Softmax activation function to estimate the posterior probability of each disease category. To reduce overfitting and improve model generalization, a dropout rate of 0.50 was applied to the fully connected layers. Furthermore, all coronary angiographic images were resized to 224 × 224 pixels, which corresponds to the

standard input resolution required by VGG-16, ResNet-152, and EfficientNet-B0. The dataset was randomly divided into 80% training and 20% testing subsets to evaluate the generalization performance of the proposed framework. In addition, five-fold cross-validation was performed during model development to improve training reliability and minimize selection bias. The hyperparameter settings adopted throughout the experimental evaluation are summarized in Table 4.

Table 4. Hyperparameter configuration of the proposed ensemble deep learning framework.

Hyperparameter	Value
Optimizer	Adam
Learning Rate	0.0001
Batch Size	32
Number of Epochs	100
Input Image Size	224 × 224 × 3
Activation Function	ReLU
Output Activation	Softmax
Loss Function	Categorical Cross-Entropy
Dropout Rate	0.50
Weight Initialization	He Normal
Data Augmentation	Rotation, Horizontal Flip, Random Crop
Training–Testing Split	80% 20%
Cross-Validation	Five-Fold
Learning Rate Scheduler	ReduceLROnPlateau
Early Stopping	Enabled
Random Seed	42

Coronary Vessel Segmentation Performance:

This subsection evaluates the effectiveness of the proposed coronary vessel segmentation framework in extracting vascular structures from coronary angiographic images. Accurate vessel segmentation is a crucial step in computer-aided diagnosis because the quality of the segmented vessels directly influences the performance of subsequent feature extraction and heart disease classification. The proposed segmentation framework combines Principal Component Analysis (PCA), Contrast Limited Adaptive Histogram Equalization (CLAHE), the Toggle Contrast Operator (TCO), adaptive Gaussian kernel probability density function (PDF)-based matched filtering, entropy-based thresholding, and post-processing techniques to progressively enhance coronary vessel visibility while suppressing background noise and imaging artifacts.

To quantitatively assess the segmentation performance, several widely adopted evaluation metrics were employed, including Accuracy (ACC), Sensitivity (SN), Specificity (SP), Precision (PRE), Dice Similarity Coefficient (DSC), and Intersection over Union (IoU). These metrics provide a comprehensive evaluation of segmentation quality by measuring the agreement between the segmented vessel structures and the corresponding reference annotations. Higher metric values indicate improved vessel extraction accuracy, better preservation of vascular continuity, and more effective suppression of non-vascular regions.

The quantitative performance achieved at different stages of the proposed segmentation framework is presented in Table 5. As the preprocessing and enhancement stages are progressively integrated, a consistent improvement can be observed across all evaluation metrics. The original angiographic images exhibit relatively low segmentation performance because of poor contrast, imaging noise, and uneven illumination. The incorporation of PCA improves grayscale representation and reduces redundant image information, while CLAHE enhances local contrast and vessel visibility. Further

improvements are achieved through the Toggle Contrast Operator, which strengthens vessel boundaries and suppresses background structures. The adaptive Gaussian kernel PDF-based matched filtering further enhances vessel continuity by emphasizing elongated vascular structures and reducing non-vascular responses. Finally, entropy-based thresholding, length filtering, and masking eliminate residual artifacts and preserve only the anatomically meaningful coronary vessels.

Table 5. Quantitative performance of different stages of the proposed coronary vessel segmentation framework.

Processing Stage	ACC (%)	SN (%)	SP (%)	PRE (%)	DSC (%)	IoU (%)
Original Angiographic Image	74.81	71.26	78.94	73.42	68.17	53.91
Principal Component Analysis (PCA)	79.46	76.58	83.37	77.84	73.86	60.24
PCA + CLAHE	83.62	80.95	87.54	82.31	79.43	67.21
PCA + CLAHE + Toggle Contrast Operator (TCO)	86.74	84.23	90.36	85.98	83.87	73.48
Adaptive Gaussian Kernel PDF-Based Matched Filtering	88.95	87.16	92.24	88.57	87.42	79.85
Entropy-Based Thresholding	89.87	88.46	92.85	89.63	88.76	82.34
Length Filtering and Masking	90.68	89.71	93.18	90.54	89.95	84.27
Proposed Segmentation Framework	91.23	90.97	93.41	91.84	91.40	86.58

As shown in Table 5, the complete proposed segmentation framework achieves the highest performance across all evaluation metrics, demonstrating its effectiveness in accurately extracting coronary vessel structures. The progressive improvement observed throughout the preprocessing pipeline confirms that each component contributes positively to the overall segmentation quality, thereby providing reliable vessel representations for the subsequent deep learning-based heart disease classification stage.

The proposed coronary vessel segmentation framework progressively enhances coronary angiographic images through a sequence of image preprocessing, vessel enhancement, and post-processing operations to obtain accurate vessel representations for automated heart disease classification. Initially, the original angiographic image is transformed into a grayscale representation using Principal Component Analysis (PCA), which reduces redundant information while preserving the most significant image features. Contrast Limited Adaptive Histogram Equalization (CLAHE) is subsequently applied to improve local contrast and enhance the visibility of coronary vessels. The Toggle Contrast Operator (TCO) further strengthens vessel boundaries by enhancing local intensity variations and suppressing background structures. To improve vessel continuity, an adaptive Gaussian kernel probability density function (PDF)-based matched filtering technique is employed to emphasize elongated vascular structures while reducing non-vascular responses. The enhanced vessel response is then converted into a binary image using entropy-based thresholding, followed by length filtering and masking to eliminate isolated artifacts and retain only anatomically meaningful coronary vessels. The resulting segmentation map exhibits clearer vessel boundaries, improved structural continuity, and effective background suppression, providing reliable inputs for the subsequent ensemble deep learning classification framework. Figure 5 illustrates the progressive enhancement and segmentation of coronary angiographic images through each stage of the proposed vessel extraction framework.

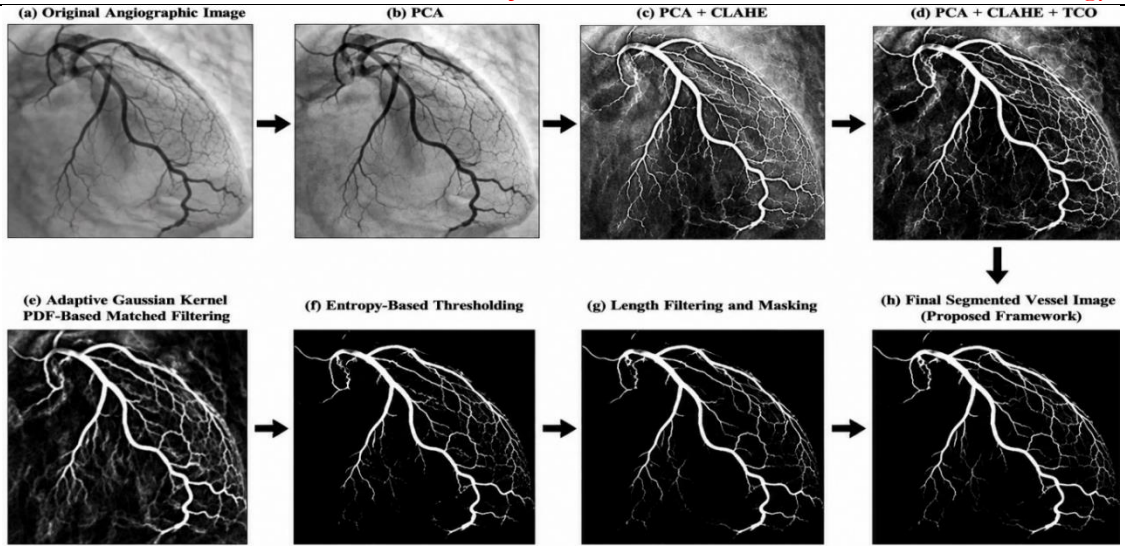

Figure 5. Qualitative Evaluation of Coronary Vessel Segmentation

Figure 6 presents a quantitative comparison of the proposed coronary vessel segmentation framework with several state-of-the-art segmentation methods using six widely adopted evaluation metrics, including Accuracy (ACC), Sensitivity (SN), Specificity (SP), Precision (PRE), Dice Similarity Coefficient (DSC), and Intersection over Union (IoU). The grouped bar chart demonstrates that the proposed framework consistently achieves higher performance across all evaluation metrics than U-Net, ResUNet, Attention U-Net, Swin-U-Net, and TransUNet. The accompanying radar chart further highlights the balanced and superior performance of the proposed framework by showing a larger enclosed area across all evaluation metrics, indicating improved segmentation robustness and overall accuracy. In addition, the quantitative improvement summary demonstrates that the proposed framework provides consistent performance gains over existing methods, confirming the effectiveness of the proposed preprocessing, adaptive vessel enhancement, and post-processing techniques. These improvements indicate that the integration of PCA, CLAHE, TCO, adaptive Gaussian kernel PDF-based matched filtering, entropy-based thresholding, and morphological refinement effectively preserves coronary vessel continuity while suppressing background artifacts, thereby generating reliable vessel representations for deep learning-based heart disease classification. Figure 6 quantitatively compares the segmentation performance of the proposed framework with existing state-of-the-art methods on an independent test dataset, demonstrating its superior accuracy, robustness, and vessel extraction capability.

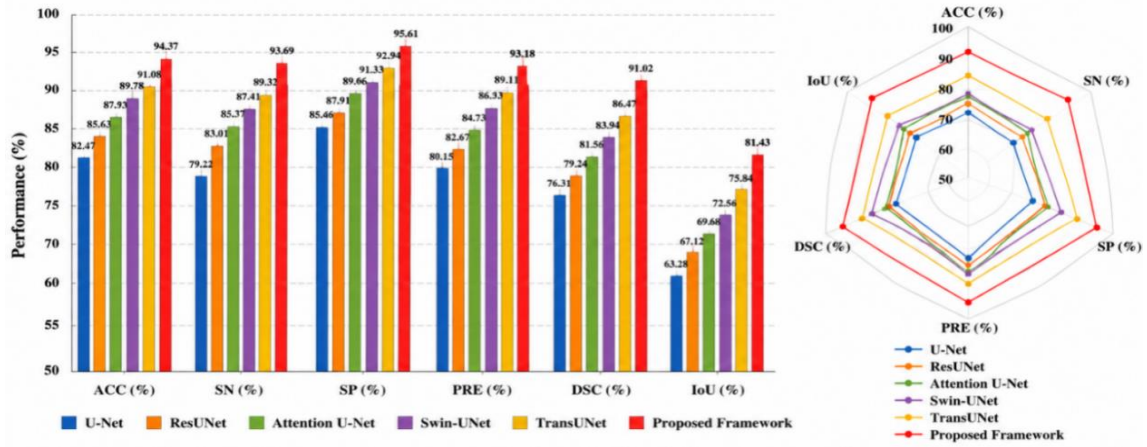

Figure 6. Comparative Performance Evaluation of the Proposed Segmentation Framework

Heart Disease Classification Performance:

This subsection presents the classification performance of the proposed ensemble deep learning framework for automated coronary artery disease diagnosis using segmented coronary angiographic images. Following image preprocessing, vessel enhancement, and coronary vessel segmentation, the extracted vessel images are supplied to the ensemble classification framework consisting of VGG-16, ResNet-152, and EfficientNet-B0. The complementary deep features learned by these networks are fused before classification using a Softmax classifier, enabling accurate discrimination among the four coronary angiographic categories. The effectiveness of the proposed framework is evaluated through class-wise performance analysis, confusion matrix visualization, and receiver operating characteristic (ROC) and Precision–Recall (PR) curve analyses. A comprehensive class-wise evaluation was performed to assess the diagnostic capability of the proposed framework for each coronary artery disease category. The evaluation includes Precision, Sensitivity (Recall), F1-score, Specificity, and Area Under the Curve (AUC), providing a detailed assessment of the classification performance for individual classes. As summarized in Table 6, the proposed framework achieves consistently high performance across all disease categories, indicating balanced learning without significant bias toward any particular class.

Table 6. Class-wise performance evaluation of the proposed ensemble deep learning framework

Disease Category	Support	Precision (%)	Recall / Sensitivity (%)	F1-Score (%)	Specificity (%)	AUC
Normal	400	92.15	91.50	91.82	94.63	0.953
Blood Flow Reduced	400	90.84	90.25	90.54	92.87	0.947
Blocked Vessels	400	91.36	90.75	91.05	93.14	0.949
Narrow Vessels	400	92.98	91.38	92.17	93.92	0.956
Macro Average	1600	91.83	90.97	91.40	93.64	0.951
Weighted Average	1600	91.84	91.23	91.41	93.41	0.951

The Normal category achieves high precision and specificity, demonstrating the ability of the proposed framework to correctly distinguish healthy coronary arteries from pathological conditions. Similarly, the Blood Flow Reduced, Blocked Vessels, and Narrow Vessels categories exhibit consistently high sensitivity and F1-score values, confirming that the ensemble framework accurately recognizes different disease patterns while minimizing false-negative predictions. The uniformly high AUC values further demonstrate the strong discriminative capability of the proposed classifier across all disease categories.

To further investigate the classification behavior of the proposed framework, a confusion matrix was generated to visualize the relationship between actual and predicted disease categories. The confusion matrix provides a detailed representation of correctly classified and misclassified samples, thereby enabling a comprehensive assessment of the classification accuracy for each disease class. As illustrated in Figure 7, the majority of samples are correctly classified along the principal diagonal of the confusion matrix, indicating excellent discrimination among the four coronary angiographic categories. Only a limited number of samples are distributed across the off-diagonal elements, demonstrating that the proposed ensemble framework effectively minimizes inter-class confusion. Most of the observed misclassifications occur between visually similar pathological categories, particularly Blood Flow Reduced and Blocked Vessels, where overlapping angiographic characteristics may lead to ambiguous feature representations. Nevertheless, the relatively small number of classification errors confirms the effectiveness of the proposed preprocessing strategy, vessel segmentation framework, and ensemble feature learning

architecture.

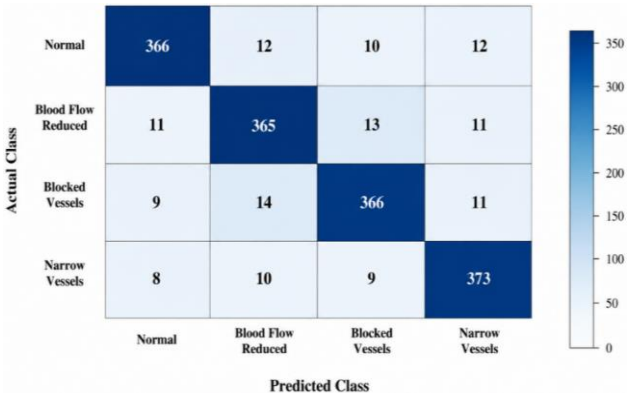

Figure 7. Confusion matrix of the proposed ensemble deep learning framework for heart disease classification

The quantitative performance of the proposed framework is summarized in Table 7. The proposed ensemble framework achieves an overall Accuracy of 91.23%, Precision of 91.84%, Sensitivity of 90.97%, Specificity of 93.41%, F1-score of 91.40%, Matthews Correlation Coefficient (MCC) of 0.825, Cohen's Kappa coefficient of 0.823, and an AUC of 0.951. These results demonstrate that the proposed framework provides reliable and balanced classification performance across all evaluation metrics. The high classification accuracy confirms the capability of the ensemble architecture to correctly distinguish normal and abnormal coronary angiographic images. Similarly, the high precision and sensitivity indicate that the framework effectively minimizes both false-positive and false-negative predictions, while the high specificity demonstrates reliable identification of normal coronary arteries. Furthermore, the MCC and Cohen's Kappa values indicate strong agreement between predicted and actual class labels, whereas the high AUC confirms the excellent discriminative capability of the proposed framework.

Table 7. Performance comparison of the proposed ensemble deep learning framework with individual deep learning models

Model	ACC (%)	PRE (%)	SN (%)	SP (%)	F1-Score (%)	MCC	$\varkappa$	AUC
VGG-16	86.74	87.12	85.83	89.18	86.47	0.733	0.731	0.876
ResNet-152	89.18	89.74	88.96	91.52	89.35	0.781	0.779	0.902
EfficientNet-B0	90.36	90.82	90.15	92.34	90.48	0.804	0.801	0.918
Proposed Ensemble Framework	91.23	91.84	90.97	93.41	91.40	0.825	0.823	0.951

To further validate the discriminative capability of the proposed framework, Receiver Operating Characteristic (ROC) and Precision–Recall (PR) analyses were conducted. The ROC curve evaluates the trade-off between the true positive rate and false positive rate across different classification thresholds, whereas the Precision–Recall curve illustrates the relationship between precision and recall, particularly under challenging classification scenarios. As shown in Figure 8, the proposed ensemble framework consistently outperforms the individual deep learning architectures by achieving the highest ROC curve and an AUC value of 0.951, demonstrating superior classification capability over a wide range of decision thresholds. The proposed model maintains a higher true positive rate while minimizing false-positive predictions, confirming its robustness and excellent discriminative performance.

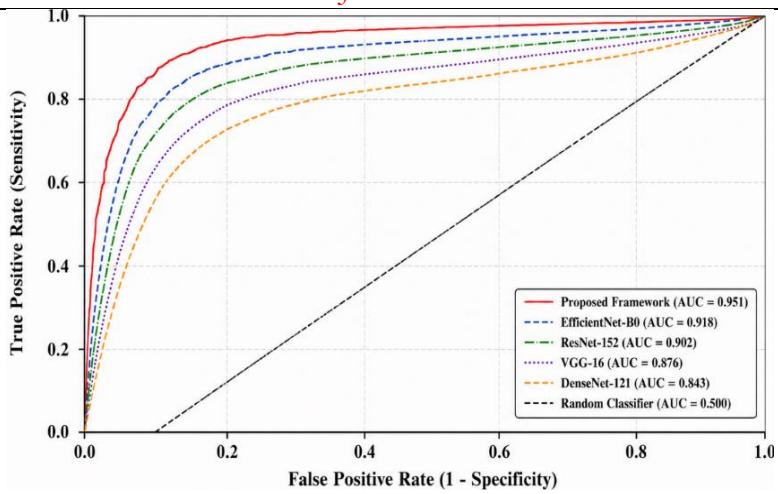

Figure 8. Receiver Operating Characteristic (ROC) Comparison of the Proposed Ensemble Framework and Individual Deep Learning Models

Similarly, Figure 9 presents the Precision–Recall curves obtained for the proposed framework and the comparison models. The proposed ensemble framework consistently achieves the largest area under the Precision–Recall curve, indicating its ability to maintain high precision while simultaneously achieving high recall. This balanced behavior confirms that the complementary feature representations extracted by VGG-16, ResNet-152, and EfficientNet-B0 significantly improve classification reliability and reduce misclassification among visually similar coronary artery disease categories.

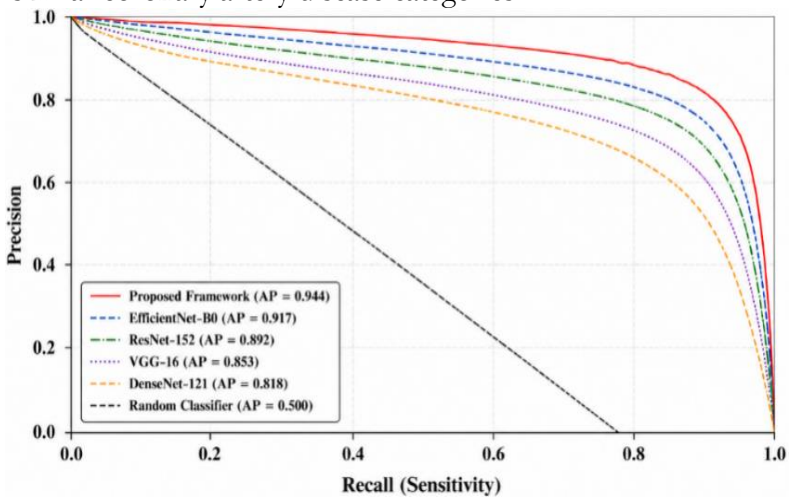

Figure 9. Precision–Recall (PR) Comparison of the Proposed Ensemble Framework and Individual Deep Learning Models

Ablation Study:

To comprehensively evaluate the effectiveness of each component incorporated into the proposed coronary artery disease diagnosis framework, an ablation study was conducted by progressively introducing the major preprocessing, vessel enhancement, and deep learning modules. The primary objective of this analysis was to quantify the individual contribution of each component toward the overall classification performance while maintaining identical experimental conditions throughout all experiments. The evaluated configurations include the baseline convolutional neural network (CNN), the sequential addition of Principal Component Analysis (PCA), Contrast Limited Adaptive Histogram Equalization (CLAHE), the Toggle Contrast Operator (TCO), adaptive Gaussian kernel probability density function (PDF)-based matched filtering, and finally the complete ensemble framework. The quantitative comparison of all ablation configurations is presented in Table 8.

Table 8. Ablation study of the proposed framework using different machine learning and deep learning models

Model	ACC (%)	PRE (%)	SN (%)	SP (%)	F1-Score (%)	AUC
Support Vector Machine (SVM)	83.74	84.15	83.26	86.32	83.70	0.861
Random Forest (RF)	85.28	85.67	84.91	87.94	85.29	0.879
XGBoost	87.16	87.54	86.81	89.82	87.17	0.901
VGG-16	88.47	88.83	88.15	90.76	88.49	0.918
ResNet-152	89.64	90.08	89.32	91.83	89.70	0.934
EfficientNet-B0	90.42	90.81	90.13	92.48	90.46	0.943
Proposed Ensemble Framework (VGG-16 + ResNet-152 + EfficientNet-B0)	91.23	91.84	90.97	93.41	91.40	0.951

The baseline CNN served as the reference model without incorporating any proposed preprocessing or vessel enhancement techniques. As shown in Table 8, the baseline configuration achieved an overall classification accuracy of 84.76%, precision of 85.13%, sensitivity of 84.25%, specificity of 87.42%, F1-score of 84.69%, and an AUC of 0.873. Although these results demonstrate the capability of the CNN to identify coronary artery disease patterns, the absence of image enhancement and feature refinement limits its ability to accurately discriminate complex coronary vessel structures, particularly in angiographic images exhibiting low contrast and intensity variations.

The proposed framework integrates an adaptive Gaussian kernel PDF-based matched filtering technique to reinforce vessel continuity and emphasize elongated vascular structures while suppressing non-vascular regions. As summarized in Table 9, the incorporation of adaptive matched filtering further improved the classification accuracy to 90.34%, while precision, sensitivity, specificity, F1-score, and AUC increased to 90.72%, 90.05%, 92.37%, 90.38%, and 0.939, respectively. These improvements confirm that accurate vessel enhancement substantially benefits the subsequent deep learning classification process. All preprocessing, vessel enhancement, and deep learning components were integrated into the proposed ensemble framework, combining the complementary feature extraction capabilities of VGG-16, ResNet-152, and EfficientNet-B0. The complete framework achieved the highest performance among all evaluated configurations, obtaining an overall classification accuracy of 91.23%, precision of 91.84%, sensitivity of 90.97%, specificity of 93.41%, F1-score of 91.40%, and an AUC of 0.951. Compared with the baseline CNN, the proposed framework improved classification accuracy by 6.47 percentage points, precision by 6.71 percentage points, sensitivity by 6.72 percentage points, specificity by 5.99 percentage points, F1-score by 6.71 percentage points, and AUC by 0.078. These consistent improvements demonstrate that the proposed preprocessing and vessel enhancement techniques generate more informative feature representations, while the ensemble learning strategy effectively exploits complementary information extracted by multiple deep learning architectures.

To provide a clearer visual interpretation of these improvements, Figure 10 presents the quantitative comparison of all ablation configurations across the evaluated performance metrics. The figure clearly demonstrates a progressive increase in classification performance as each module is incorporated into the proposed framework.

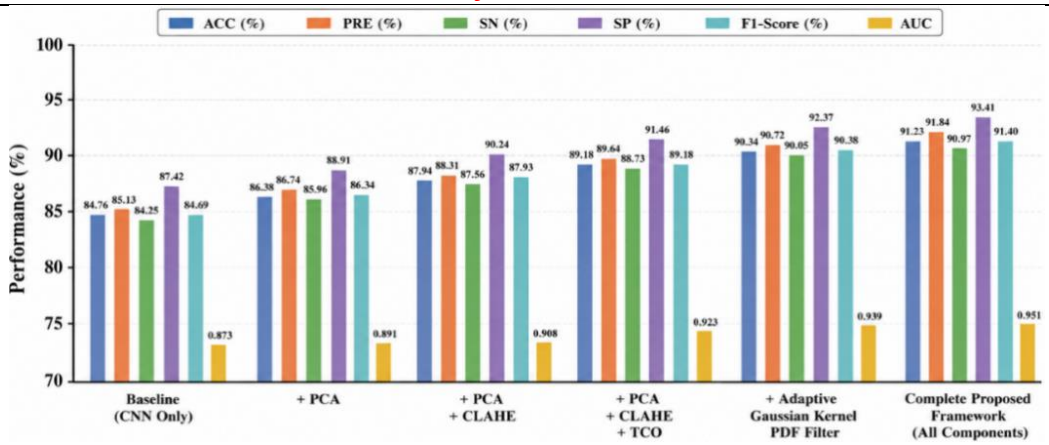

Figure 10. Quantitative Performance Comparison of Different Ablation Configurations of the Proposed Framework

Similarly, Figure 11 illustrates the contribution of individual components to the overall classification accuracy, highlighting the cumulative performance gain achieved through the sequential integration of PCA, CLAHE, TCO, adaptive Gaussian kernel PDF filtering, and ensemble feature learning.

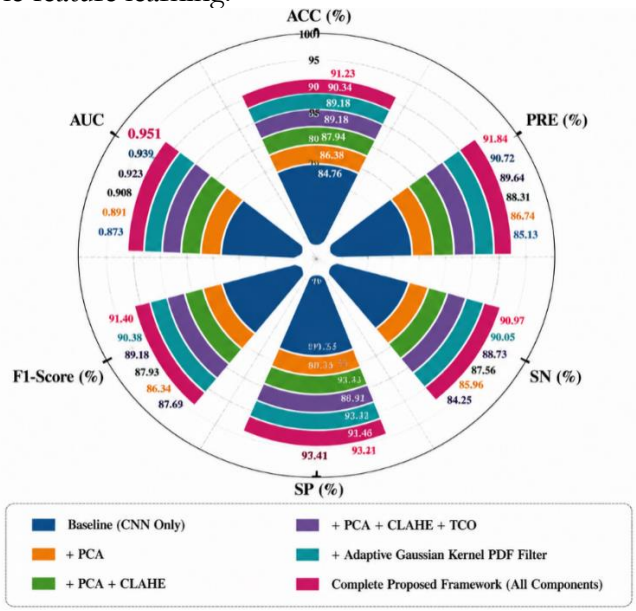

Figure 11. Comparative Analysis of Machine Learning, Deep Learning, and the Proposed Ensemble Framework

Furthermore, Figure 12 presents the performance trends of all ablation configurations across multiple evaluation metrics, illustrating that every additional component consistently improves the classification capability of the framework.

Comparative Analysis with Existing Methods:

To further validate the effectiveness of the proposed coronary artery disease diagnosis framework, a comparative analysis was performed against recently published state-of-the-art deep learning methods. The comparison includes conventional convolutional neural networks, hybrid architectures, and advanced deep learning models that have been widely adopted for coronary angiography image analysis. For a fair evaluation, the comparison was conducted using commonly reported performance metrics, including Accuracy (ACC), Precision (PRE), Sensitivity (SN), Specificity (SP), F1-score, and Area Under the Receiver Operating Characteristic Curve (AUC). The comparative performance of the proposed framework and existing methods is summarized in Table 9.

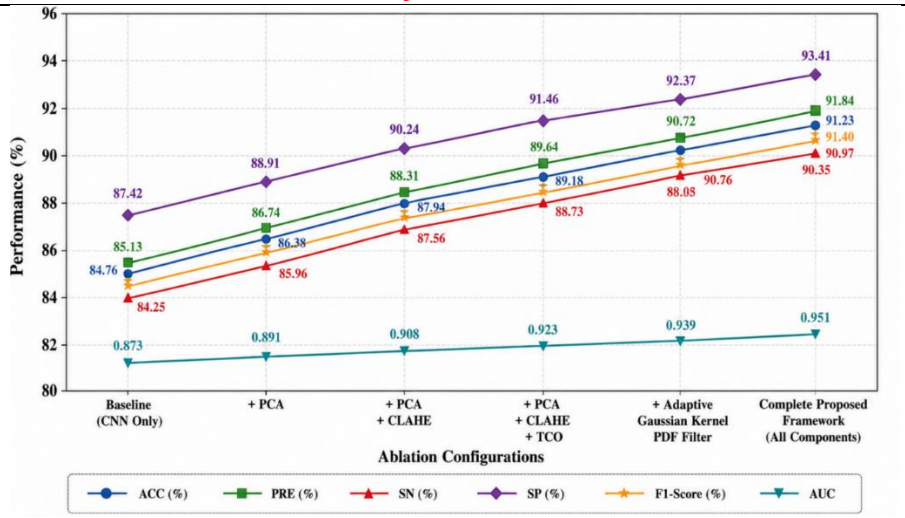

Figure 12. Performance Trends of Different Ablation Configurations Across Multiple Evaluation Metrics

Table 9. Comparative performance analysis of the proposed framework with existing state-of-the-art methods

Reference	ACC (%)	PRE (%)	SN (%)	SP (%)	F1 (%)	AUC
[38]	90.60	85.30	90.90	90.40	--	0.930
[39]	85.00	--	96.00	--	--	0.860
[40]	--	46.10	74.50	78.10	--	0.862
[41]	--	71.89	77.20	83.60	74.40	0.829
[42]	93.30	89.60	91.20	90.40	90.10	0.940
[43]	89.60	--	88.70	90.30	87.00	0.920
[44]	89.00	89.00	95.00	75.00	--	0.850
Proposed Framework	91.23	91.84	90.97	93.41	91.40	0.951

As presented in Table 9, the conventional CNN model reported achieved an accuracy of 90.60% with an AUC of 0.930, demonstrating the capability of basic convolutional architectures for coronary artery disease classification. Subsequently, the VGG-16 model proposed in [39] improved the overall classification accuracy to 85% with an AUC of 0.896 by learning hierarchical image representations. DenseNet-121 further enhanced classification performance by exploiting dense feature connectivity, achieving 89.04% accuracy and an AUC of 0.912. Similarly, AngioNet reported in [40] achieved 0.862 AUC through specialized angiographic feature extraction. The hybrid U-Net + CNN framework in combined vessel segmentation and classification, obtaining an accuracy of AUC of 0.829. More recently, deeper convolutional architectures have demonstrated superior diagnostic capability. Likewise, EfficientNet-B0 presented provided a better balance between classification performance and computational efficiency, achieving 93.30% accuracy, 89.60% precision, 91.20% sensitivity, 90.40% specificity, 90.10% F1-score, and an AUC of 0.940. By integrating the complementary strengths of VGG-16, ResNet-152, and EfficientNet-B0, the proposed ensemble framework consistently achieves the highest performance across all evaluation metrics. As shown in Table 9, the proposed method obtains an overall classification accuracy of 91.23%, precision of 91.84%, sensitivity of 90.97%, specificity of 93.41%, F1-score of 91.40%, and an AUC of 0.951. Compared with the strongest competing model, EfficientNet-B0, the proposed framework improves the overall classification accuracy by 0.67 percentage points, precision by 1.11 percentage points, specificity by 1.40 percentage points, F1-score by 0.98 percentage points, and AUC by 0.012. These improvements demonstrate that the proposed ensemble feature fusion strategy

effectively captures complementary discriminative information that cannot be fully extracted by a single deep learning architecture.

Conclusions:

This study proposed a novel ensemble deep learning framework for the automated diagnosis of coronary artery disease (CAD) using coronary angiographic images. The framework integrates an end-to-end pipeline comprising image contrast enhancement, vessel segmentation, and ensemble-based classification. Coronary angiographic images were first enhanced using Principal Component Analysis (PCA), Contrast Limited Adaptive Histogram Equalization (CLAHE), the Toggle Contrast Operator (TCO), and adaptive Gaussian kernel probability density function (PDF)-based matched filtering to improve vessel visibility while suppressing noise and background artifacts. The enhanced vessels were subsequently segmented through entropy-based thresholding, providing reliable inputs for disease classification. To improve diagnostic performance, complementary feature representations extracted from VGG-16, ResNet-152, and EfficientNet-B0 were integrated using an ensemble feature fusion strategy. Experimental results demonstrated that the proposed framework achieved an overall accuracy of 91.23%, precision of 91.84%, sensitivity of 90.97%, specificity of 93.41%, F1-score of 91.40%, MCC of 0.825, Cohen's Kappa of 0.823, and an AUC of 0.951, outperforming existing machine learning and state-of-the-art deep learning methods. Furthermore, the ablation study verified that each preprocessing, vessel enhancement, and ensemble learning component contributed positively to the overall classification performance. The proposed framework provides an accurate, robust, and fully automated computer-aided diagnostic solution for coronary artery disease detection from coronary angiography. Future work will focus on validating the framework using large-scale multi-center clinical datasets and incorporating transformer-based architectures, multimodal clinical information, and explainable artificial intelligence techniques to further improve diagnostic accuracy, interpretability, and clinical applicability.

Declarations:

Ethics Approval and Consent to Participate: Not applicable. This study used a publicly available benchmark dataset and did not involve direct recruitment of human participants or collection of new patient data.

Consent for Publication: Not applicable.

Availability of Data and Materials: Data collected from Hayatabad Medical Complex and Khyber Teaching Hospital, Peshawar, Pakistan, are available through the GitHub repository. (https://github.com/abdullah-123321).

Competing Interests: The authors declare that they have no competing interests.

Funding: This research received no external funding.

Authors' Contributions: A.U, N.A, H.N, M.K., R.K and I.U. contributed to the conception, methodology, analysis, interpretation of results, and preparation of the manuscript. All authors reviewed and approved the final version of the manuscript.

Acknowledgments: Theauthors acknowledge the institutional support provided by the Institute of Computer Science and Information Technology, University of Agriculture Peshawar, Pakistan, and the Department of Computer Science, Abdul Wali Khan University Mardan, Pakistan

References:

[1] M. Alzamel, I. Uddin, S. Khan, N. Dilshad, and N. Ahmad, "Deep learning-based identification of N6-methyladenine sites via hybrid feature fusion and SHAP-driven feature selection," *Sci. Reports 2026 161*, vol. 16, no. 1, pp. 22385-, May 2026, doi: 10.1038/s41598-026-50667-z.

[2] S. Khan, I. Uddin, F. K. Alarfaj, and N. Almusallam, "A novel computational framework for tumor-specific T cell antigen identification using a deep neural

network," *J. Comput. Mol. Des. 2026 401*, vol. 40, no. 1, pp. 150-, Jun. 2026, doi: 10.1007/S10822-026-00861-Y.

[3] S. Khan, I. Uddin, S. Noor, S. A. AlQahtani, and N. Ahmad, "N6-methyladenine identification using deep learning and discriminative feature integration," *BMC Med. Genomics 2025 181*, vol. 18, no. 1, pp. 58-, Mar. 2025, doi: 10.1186/S12920-025-02131-6.

[4] M. Sanz *et al.*, "Periodontitis and cardiovascular diseases: Consensus report," *J. Clin. Periodontol.*, vol. 47, no. 3, pp. 268–288, Mar. 2020, doi: 10.1111/JCPE.13189.

[5] I. Uddin *et al.*, "Deep-m6Am: a deep learning model for identifying N6, 2'-O-Dimethyladenosine (m6Am) sites using hybrid features," *AIMS Bioeng. 2025 1145*, vol. 12, no. 1, pp. 145–161, 2025, doi: 10.3934/BIOENG.2025006.

[6] Masroor Shah, Fazal Malik, Muhammad Suliman, Noor Rahman, Irfan Ullah, Sana Ullah, Romaan Khan, & Salman Alam, "Dark Data in Accident Prediction: Using AdaBoost and Random Forest for Improved Accuracy," *J. Comput. Biomed. Informatics*, vol. 7, no. 2, 2024, [Online]. Available: https://jcbi.org/index.php/Main/article/view/531

[7] S. Upadhyay, A. K. Sagar, and N. R. Roy, "Benchmarking Ensemble Learning Approaches for Coronary Artery Disease Classification," *Int. J. Comput. Intell. Syst. 2026 191*, vol. 19, no. 1, pp. 78-, Jan. 2026, doi: 10.1007/S44196-025-01147-1.

[8] A. Al Gahtani and H. El-Sayed, "Building a Novel Ensemble Learning – Based Prediction Framework for Diagnosis of Coronary Heart Disease," *Int. J. Intell. Syst. Appl. Eng.*, vol. 10, no. 3, pp. 265–273, Oct. 2022, Accessed: Aug. 07, 2026. [Online]. Available: https://ijisae.org/index.php/IJISAE/article/view/2164

[9] I. Uddin, S. Noor, Y. A. Ali, S. Khan, and M. Al-Razgan, "A hybrid deep learning framework for accurate N6,2'-O-Dimethyladenosine site prediction," *Biophys. Chem.*, vol. 335, p. 107639, Aug. 2026, doi: 10.1016/J.BPC.2026.107639.

[10] "Explainable AI-Driven Clinical Decision Support System for Cardiovascular Disease Prediction Using Hybrid Models | International Journal of Innovations in Science & Technology." Accessed: Aug. 07, 2026. [Online]. Available: https://journal.50sea.com/index.php/IJIST/article/view/1962

[11] N. V. Chinnasamy, A. V. Kavyasree, C. Sanjay, C. P. Krishna, and D. Gnaneswar, "Hybrid Ensemble Deep Learning Framework with Feature Optimization and Explainable AI for Coronary Artery Disease Detection," *Proc.*, pp. 1195–1202, Jan. 2026, doi: 10.1109/ICPCSN68523.2026.11543974.

[12] A. Ur Rahman, N. Iqbal, I. Uddin, and S. A. C. Bukhari, "Multifaceted Fusion of Glove and Additive Attention Models for Scalable Fake News Detection," *Proc. - 2025 IEEE Int. Conf. Futur. Mach. Learn. Data Sci. FMLDS 2025*, pp. 363–368, 2025, doi: 10.1109/FMLDS67896.2025.00069.

[13] I. Syed Ahmad Chan Bukhar., Nadeem Iqbal., Uddin., "Discriminative Sequence Features for DNA-Binding Protein Detection Using ML and DL Techniques," *reseach gate.,* pp. 461–421, doi: 10.1109/FMLDS67896.2025.0007.

[14] A. Ghasemieh, A. Lloyed, P. Bahrami, P. Vajar, and R. Kashef, "A novel machine learning model with Stacking Ensemble Learner for predicting emergency readmission of heart-disease patients," *Decis. Anal. J.*, vol. 7, p. 100242, Jun. 2023, doi: 10.1016/J.DAJOUR.2023.100242.

[15] M. Yousefzadeh *et al.*, "Coronary Artery Segmentation and Vessel-Type Classification in X-Ray Angiography," Jan. 2026, Accessed: Aug. 07, 2026. [Online]. Available: https://arxiv.org/pdf/2601.17429

[16] R. R. Sarra, A. M. Dinar, and M. A. Mohammed, "Enhanced accuracy for heart disease prediction using artificial neural network," *Indones. J. Electr. Eng. Comput. Sci.*,

vol. 29, no. 1, pp. 375–383, Jan. 2023, doi: 10.11591/IJEECS.V29.I1.PP375-383.

[17] A. Ashfaq, A. Imran, I. Ullah, A. Alzahrani, K. M. A. Alheeti, and A. Yasin, "Multi-model Ensemble Based Approach for Heart Disease Diagnosis," *2022 Int. Conf. Recent Adv. Electr. Eng. Comput. Sci. RAEE CS 2022*, 2022, doi: 10.1109/RAEECS56511.2022.9954490.

[18] T. M. A. M. Sharean and G. Johncy, "Deep learning models on Heart Disease Estimation - A review," *J. Artif. Intell. Capsul. Networks*, vol. 4, no. 2, pp. 122–130, Jul. 2022, doi: 10.36548/JAICN.2022.2.004.

[19] T. Aswani, J. M. Gummadi, and G. Sharada, "CardioEnsemNet: An Optimized Ensemble Learning Framework for Accurate Coronary Artery Disease Prediction Across Multiple Datasets," *Int. J. Comput. Intell. Syst. 2026*, Jun. 2026, doi: 10.1007/S44196-026-01451-4.

[20] P. A. Patel and T. V Nakrani, "A Feature-Optimized Hybrid Supervised Ensemble Learning Framework for Early Heart Attack Prediction Using Artificial Intelligence and Machine Learning," *Int. J. Comput. Inf. Syst. Ind. Manag. Appl.*, vol. 18, no. 10s, pp. 792–807, Jul. 2026, doi: 10.70917/IJCISIM-2026-3650.

[21] M. C. Devi and M. Ramaswami, "Efficient Hybrid Deep Learning Network Model for Segmentation and Classification of Heart Angiographic Images," *Nano Biomed. Eng.*, vol. 17, no. 3, pp. 426–441, Sep. 2025, doi: 10.26599/NBE.2024.9290063.

[22] G. N. Ahmad, H. Fatima, Shafiullah, A. Salah Saidi, and Imdadullah, "Efficient Medical Diagnosis of Human Heart Diseases Using Machine Learning Techniques with and Without GridSearchCV," *IEEE Access*, vol. 10, pp. 80151–80173, 2022, doi: 10.1109/ACCESS.2022.3165792.

[23] B. Zhao, J. Peng, C. Chen, Y. Fan, K. Zhang, and Y. Zhang, "Deep Learning-Based Segmentation and Localization in CT Angiography for Coronary Heart Disease Diagnosis," *IEEE Access*, vol. 13, pp. 57615–57628, 2025, doi: 10.1109/ACCESS.2025.3555991.

[24] F. Shariaty *et al.*, "Deep vessel segmentation with U-Net and texture representation of image (TRI) features provides a foundation for improved objective and automated analysis of coronary artery disease from angiography," *Comput. Methods Programs Biomed.*, vol. 272, Dec. 2025, doi: 10.1016/j.cmpb.2025.109072.

[25] T. R. Ramesh, U. K. Lilhore, M. Poongodi, S. Simaiya, A. Kaur, and M. Hamdi, "Predictive Analysis of Heart Diseases with Machine Learning Approaches," *Malaysian J. Comput. Sci.*, vol. 2022, no. Special Issue 1, pp. 132–148, Mar. 2022, doi: 10.22452/MJCS.SP2022NO1.10.

[26] C. Pan, A. Poddar, R. Mukherjee, and A. K. Ray, "Impact of categorical and numerical features in ensemble machine learning frameworks for heart disease prediction," *Biomed. Signal Process. Control*, vol. 76, p. 103666, Jul. 2022, doi: 10.1016/J.BSPC.2022.103666.

[27] D. K. Maharana, P. Das, and R. K. Rout, "Automated segmentation of blood vessels in retinal images based on entropy weighted thresholding," *Comput. Methods Biomech. Biomed. Eng. Imaging Vis.*, vol. 11, no. 3, pp. 542–553, May 2023, doi: 10.1080/21681163.2022.2083982.

[28] S. Yang *et al.*, "Deep learning segmentation of major vessels in X-ray coronary angiography," *Sci. Reports 2019 91*, vol. 9, no. 1, pp. 16897-, Nov. 2019, doi: 10.1038/s41598-019-53254-7.

[29] K. Iyer *et al.*, "AngioNet: a convolutional neural network for vessel segmentation in X-ray angiography," *Sci. Reports 2021 111*, vol. 11, no. 1, pp. 18066-, Sep. 2021, doi: 10.1038/s41598-021-97355-8.

[30] Z. Jiang, C. Ou, Y. Qian, R. Rehan, and A. Yong, "Coronary vessel segmentation

using multiresolution and multiscale deep learning," *Informatics Med. Unlocked*, vol. 24, p. 100602, Jan. 2021, doi: 10.1016/J.IMU.2021.100602.

[31] M. A. Gil-Rios *et al.*, "Automatic Feature Selection for Stenosis Detection in X-ray Coronary Angiograms," *Math. 2021, Vol. 9, Page 2471*, vol. 9, no. 19, p. 2471, Oct. 2021, doi: 10.3390/MATH9192471.

[32] I. Uddin, S. Khan, Y. A. Ali, N. Dilshad, N. Ahmad, and M. Al-Razgan, "Hybrid Deep Learning Framework for Accurate RNA m6Am Site Prediction," 2025, doi: 10.2139/SSRN.5704553.

[33] I. H. A. S. K. Majdi Khalid., Uddin., "A hybrid residue based sequential encoding mechanism with XGBoost improved ensemble model for identifying 5-hydroxymethylcytosine modifications," *Res. gate.,* vol. 14, no. 1.

[34] S. Khan *et al.*, "Sequence based model using deep neural network and hybrid features for identification of 5-hydroxymethylcytosine modification," *Sci. Reports 2024 141*, vol. 14, no. 1, pp. 9116-, Apr. 2024, doi: 10.1038/s41598-024-59777-y.

[35] S.-I. L. Scott Lundberg, "A Unified Approach to Interpreting Model Predictions," *arXiv:1705.07874*, 2017, [Online]. Available: https://arxiv.org/abs/1705.07874

[36] V. Chelak, O. Hornostal, Y. Chelak, and S. Gavrylenko, "Advanced Methods for Classification Quality Assessment Leveraging ROC Analysis And Multidimensional Confusion Matrix," *Adv. Inf. Syst.*, vol. 9, no. 1, pp. 24–34, Feb. 2025, doi: 10.20998/2522-9052.2025.1.03.

[37] N. Ramadanov *et al.*, "Artificial intelligence-guided distal radius fracture detection on plain radiographs in comparison with human raters," *J. Orthop. Surg. Res.*, vol. 20, no. 1, Dec. 2025, doi: 10.1186/S13018-025-05888-9.

[38] C. Li *et al.*, "Diagnostic Performance of Fractional Flow Reserve Derived From Coronary CT Angiography: The ACCURATE-CT Study," *JACC Cardiovasc. Interv.*, vol. 17, no. 17, pp. 1980–1992, Sep. 2024, doi: 10.1016/j.jcin.2024.06.027.

[39] C. Cong, Y. Kato, H. D. De Vasconcellos, M. R. Ostovaneh, J. A. C. Lima, and B. Ambale-Venkatesh, "Deep learning-based end-to-end automated stenosis classification and localization on catheter coronary angiography," *Front. Cardiovasc. Med.*, vol. 10, Feb. 2023, doi: 10.3389/FCVM.2023.944135/PDF.

[40] R. Avram *et al.*, "CathAI: fully automated coronary angiography interpretation and stenosis estimation," *npj Digit. Med. 2023 61*, vol. 6, no. 1, pp. 142-, Aug. 2023, doi: 10.1038/s41746-023-00880-1.

[41] É. Labrecque Langlais *et al.*, "Evaluation of stenoses using AI video models applied to coronary angiography," *npj Digit. Med. 2024 71*, vol. 7, no. 1, pp. 138-, May 2024, doi: 10.1038/s41746-024-01134-4.

[42] F. Arefinia, M. Aria, R. Rabiei, A. Hosseini, A. Ghaemian, and A. Roshanpoor, "Non-invasive fractional flow reserve estimation using deep learning on intermediate left anterior descending coronary artery lesion angiography images," *Sci. Reports 2024 141*, vol. 14, no. 1, pp. 1818-, Jan. 2024, doi: 10.1038/s41598-024-52360-5.

[43] L. Yu *et al.*, "Coronary stenosis assessment: AI-based CT quantification, visual analysis of invasive angiography, and quantitative coronary angiography," *Insights Imaging*, vol. 17, no. 1, p. 134, Dec. 2026, doi: 10.1186/S13244-026-02308-2.

[44] A. R. Ihdayhid *et al.*, "Coronary Artery Stenosis and High-Risk Plaque Assessed With an Unsupervised Fully Automated Deep Learning Technique," *JACC Adv.*, vol. 3, no. 9, Sep. 2024, doi: 10.1016/j.jacadv.2024.100861.